RESEARCH

MEASUREMENT OF THE EFFICIENCY OF EVACUATED TUBE SOLAR COLLECTORS UNDER VARIOUS OPERATING CONDITIONS

S. E. Zubriski[1] and K. J. Dick[2]

ABSTRACT

The operating efficiency of evacuated tubes themselves under varying environmental conditions and installation scenarios, independent of water and space heating auxiliary equipment, are not readily available values. Further, Manitoba specific data has not been established. The purpose of this research program was to measure the efficiency of evacuated tube solar collectors under various operating conditions including: the angle of inclination towards the incident solar radiation, heat transfer fluid flow rate, glazing installation, and number of evacuated tubes. The operating conditions and configurations were chosen to represent realistic or probable installation scenarios and environmental conditions. Furthermore, the research aimed to identify the suitability of evacuated tube solar collectors to each of the scenarios. These design values are of use for appropriate sizing of water or space heating systems, system configuration and optimization, and calculation of return on investment. The scope of the research project was limited to the efficiency of various configurations of a 32-tube panel, not the entire solar domestic hot water or space heating system. Thus, factors such as heat loss in the tubing, solar storage tank, and heat exchanger efficiency were not investigated. The findings indicated that efficiency varied by approximately 5% between the different collector configurations, as observed from the overlay graph of results. When the efficiency of a collector is considered within a system it is proposed that effectiveness may be a better measure of overall performance.

KEYWORDS

solar collector, evacuated tube, solar hot water

[1]Graduate Student, Department of Biosystems Engineering, University of Manitoba, Winnipeg, Canada.
[2]Associate Professor, Director of the Alternative Village, Department of Biosystems Engineering, University of Manitoba, Winnipeg, Canada, kjdick@ms.umanitoba.ca.
*See Appendix for Nomenclature.

INTRODUCTION

In Canada, approximately 80% of residential energy consumption is apportioned to domestic hot water and space heating applications (Sibbitt et al. 2007). A common, unsubstantiated barrier to large-scale adoption of solar heating technologies for domestic hot water and space heating is the relative lack of sunshine during the fall and winter months when heating demand is high (Sibbitt et al. 2007). According to Kemp (2005), on average, Manitoba residents can expect to obtain approximately 56% of the energy required for water heating purposes from solar thermal sources, while those as far north as Inuvik in the Northwest Territories can expect approximately 33%. These statistics indicate that even the most northerly locations with extremely cold climates and minimal solar radiation are able to benefit from solar water heating technologies.

The purpose of this research program was to measure the performance of a heat-pipe type evacuated tube solar collectors in the northern prairie climate of Manitoba under various operating conditions and configurations. Often, system efficiencies are measured in laboratories under artificial illumination, not taking into account environmental conditions such as cloud cover, visibility, shading, wind, and ambient outdoor temperature. In addition, the operating efficiency of the evacuated tubes themselves under varying environmental conditions and installation scenarios, independent of water and space heating auxiliary equipment, are not readily available values. Further, Manitoba specific data has not been established. These design values would be of use for appropriate sizing of water or space heating systems, system configuration and optimization, and calculation of return on investment.

The sun provides energy to our planet at a rate of 1367 W/m^2, as measured outside of the earth's atmosphere. Referred to as the solar constant, G_{sc} is defined as "the energy from the sun per unit time received on a unit area of surface perpendicular to the direction of propagation of the radiation at mean earth-sun distance outside of the atmosphere" (Duffie and Beckman 2006). While solar energy may be free for the taking, particular challenges are encountered in the effective collection and storage of this energy. Numerous authors (Duffie and Beckman 2006; Kalogirou 2004; Morrison et al. 2004) note that evacuated tube collectors have much greater efficiencies than the common flat plate collector, especially at times of cold temperature and low insolation.

Evacuated tube collectors vary widely in their construction and operation (Morrison et al. 2004). A number of factors can affect collector performance such as slope of tubes, flow rate and dust or covering. Weiss (2003) indicates that collector tilt angle range of 30° to 75° has little effect on overall performance. The baseline collector and two others in this study at 45° and directed due south. The fourth panel was vertical. Weiss (2003) also notes that a vertically mounted south facing panel has only 20% less fractional savings then one placed optimally. El-Nashar (1994) found that the accumulation of dust on tubes can potentially reduce performance to between 60–70% of optimum.

A number of standard test procedures exist for the determination of system efficiency as it pertains to solar domestic hot water systems. Although this specific research pertains to the efficiency of the evacuated tubes themselves, these standards provide basic guidelines and many useful recommendations.

A number of test methods for the evaluation of solar hot water systems were reviewed. The International Standard Organization (ISO) ISO 9459-2 and 9459-5 have been used by Carvalho and Naron 2001, Marshall 1999, and Morrison et al. 2003.

The Canadian Standards Association's (CSA) CAN/CSA-F379.1-88 (1988a) is concerned with the performance, durability, and safety of packaged solar domestic hot water systems, as proposed by a manufacturer, designed for use in small buildings. The purpose of this thermal test is "to determine the net solar energy delivered by a system when tested under simulated standard weather and load conditions representative of year-round operation of the system" (CAN/CSA 1988a).

CAN/CSA-F378-87 (1988b) is more specific in its intentions than CAN/CSA-F379.1-88, noting that it is applicable to solar collectors capable of converting solar energy into thermal energy, including such technologies as glazed and unglazed flat plate collectors, vacuum envelope collectors, concentrating collectors, and boiling/condensing collectors. Unlike CAN/CSA-F379.1-88, this standard allows for outdoor testing of the apparatus, outlining the requirements for set-up, providing that indoor testing is prohibitive.

Both CAN/CSA-F378-87 and CAN/CSA-F379.1-88 reference ANSI/ASHRAE Standards 93 and 95. The approach used for this research used ASHRAE Standard 93-2003: Methods of Testing to Determine the Thermal Performance of Solar Collectors. This was considered to be appropriate since the water and propylene glycol heat-transfer fluid did not change phase in the system.

The aim of this research was to evaluate the performance of heat-tube type evacuated tube solar hot water systems with respect to collector angle, flow rate and plastic covering of the tubes.

RESEARCH PROGRAM

The scope of the research project was limited to the efficiency of various configurations of a 32-tube panel, not the entire solar domestic hot water or space heating system. Thus, factors such as heat loss in the tubing, solar storage tank, and heat exchanger efficiency were not investigated.

The evacuated tube collectors used in this research project were designed and manufactured by Copperhill Alternate Energy Inc. The TM-32 collectors consist of 32 all-glass tubes with a stainless steel manifold mounted on a stainless steel frame. The condenser ends of the evacuated tubes seat into sockets in a copper manifold inside of a polyurethane foam and fiberglass insulated stainless steel header cylinder. The header is 2.215 metres in length and 0.170 metres in diameter. The tubes themselves are manufactured out of borosilicate glass, with an outer tube diameter of 47 mm and a length of 1.43 metres. The chemical composition of the absorptive coating is unknown as it is considered proprietary information. The total gross area of the collector is 3.429 m^2. The heat transfer fluid is a mixture of 50% propylene glycol and 50% distilled water.

The following panel configurations were used for this study:

Collector at 50° to Horizontal, Intermediate Flow Rate (Control)

Collector at 50° to Horizontal, Intermediate Flow Rate Covered with Suntuf™ corrugated polycarbonate panels

Collector at 50° to Horizontal, Increased Flow Rate

Collector at 90° to Horizontal, Low Flow Rate

Collector at 50° to Horizontal, Intermediate Flow Rate 16 Tubes Removed

These scenarios represent actual or probable installation configurations. Four collectors were erected along the south side of the Biosystems Strawbale Research Facility at the Alternative Village on the University of Manitoba Fort Garry Campus in Winnipeg. The external setup is illustrated in Figure 1 with the internal equipment shown in Figure 2. The collector angled at 50° to the horizontal with intermediate flow rate was used as the control for the experiment and it represents the base line or the standard operation and installation configuration. The efficiencies of the remaining collector configurations were compared to that of the control, and to each other in terms of overall performance. All of the collectors were erected on a scaffold system that placed them approximately 1600 mm above the ground facing due south.

The incident solar radiation, ambient outdoor temperature, indoor temperature, inlet and outlet temperatures of the manifold, and inlet and outlet temperatures of the fin-tube heat exchanger were monitored on a continual basis. The incident radiation was measured simultaneously with the condenser end of the heat pipe itself. In addition, the ambient temperature both inside and outside of the strawbale building was measured. As with Sharma et al. (2004) the incident radiation was measured with a pyranometer. A Kipp and Zonen model CMA11 pyranometer mounted approximately 4 metres above grade was used. An Agilent 34970A data acquisition switch with three 34901A -20 channel multiplexers were used to collect both the solar radiation and temperature data.

FIGURE 1. Test Setup—Exterior.

1 = Mini manifold and single evacuated tubes
2 = Panel 4
3 = Panel 3
4 = Panel 2
5 = Panel 1
6 = Manifold inlet
7 = Manifold outlet
8 = Pyranometer
9 = PEX tube runs from panels
10 = PEX tube run into bale building (through wall)
11 = Tension straps and screw pile
12 = Scaffold
13 = Platform
14 = South facing side of strawbale building

FIGURE 2. Test Setup Inside the Biosystems Strawbale Research Facility.

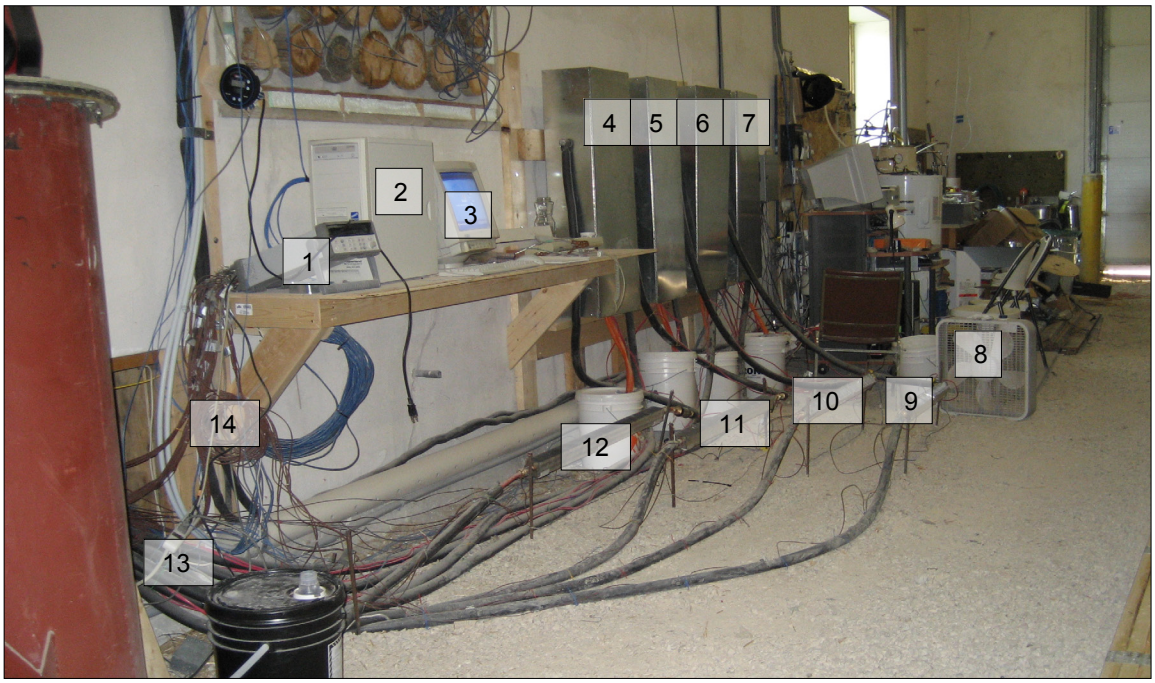

1 = Agilent data acquisition system
2 = Computer
3 = Monitor
4 = Control panel 1
5 = Control panel 2
6 = Control panel 3
7 = Control panel 4
8 = Box fan
9 = Fin tube heat exchanger 4
10 = Fin tube heat exchanger 3
11 = Fin tube heat exchanger 2
12 = Fin tube heat exchanger 1
13 = PEX tube run out of bale building (through wall)
14 = Thermocouple wire

Data were collected for approximately eighteen months, beginning in July of 2008, and concluding in January of 2010. The actual amount of time allocated to each collector configuration varied due to setup time.

Figure 3 provides a schematic of the test setup. Each of the panels were connected to a control panel that maintained system pressure and flow rates. The heat generated from the evacuated tube system was dissipated by means of a fin tube heater. With the focus on panel efficiency the authors wanted remove as much heat as possible from the system. The temperature was measured at the inlet and outlet of both the collector and the fin tube heat exchanger using T-type thermocouples. A temperature rise indicated the quantity of energy that the evacuated tube was able to extract from the incoming solar radiation, or in other words, it represented the usable energy obtained. The collector configurations are more accurate representations of the service conditions since the specific heat of the heat transfer fluid, and the ability of the condenser end to transfer energy to this fluid must be considered. Of the literature reviewed, this approach is most similar to that taken by Mathioulakis and Belessiotis (2001) in which the operation parameters of the heat-pipe itself are specifically investigated. The following summarizes the setup for each of the five configurations.

FIGURE 3. System Configuration.

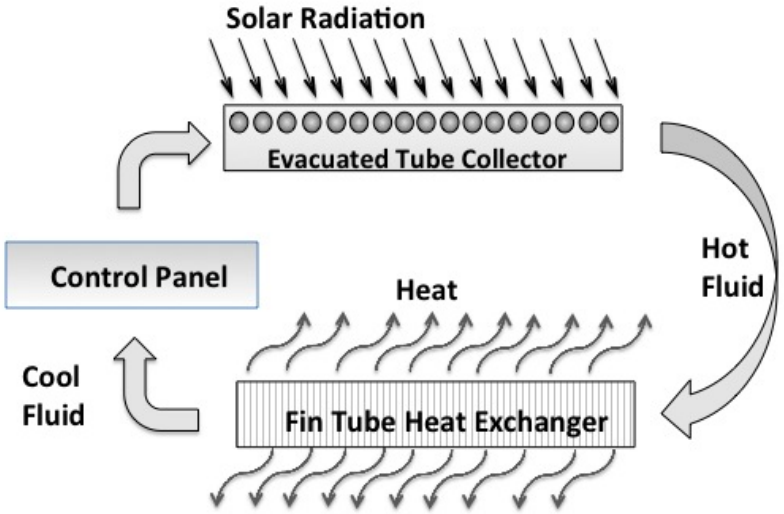

Collector 1 at 50° to Horizontal, Intermediate Flow Rate, Covered

Evidence in the literature indicates a decrease in collector efficiency as a result of dust accumulation in the summer, and snow accumulation in the winter, on the evacuated tubes. It is implied that due to the shape of the tubes and the close proximity of adjacent tubes, cleaning and snow removal may prove to be difficult. To alleviate this loss, it is proposed that a glazing material, either glass or plastic, depending on the durability and physical properties of the material, be mounted in front of the evacuated tubes, to facilitate cleaning and snow shedding. For the purposes of this investigation, Suntuf™ corrugated polycarbonate panels were installed over one evacuated tube collector and the effect on collector efficiency was measured. The intermediate pump flow rate of the Armstrong Astro 3-Speed pump, 4.92 lpm (1.3 gpm), was used.

Collector 2—Sloped at 50° Intermediate Flow Rate-Control:

This collector was the control system with a slope of 50° to the horizontal. Duffie and Beckman (2006) report that solar collectors are most efficient when mounted at an angle equal to the latitude of the site. Winnipeg is located at 50° N latitude, thus the collector was mounted at the same angle. The intermediate pump flow rate of the Armstrong Astro 3-Speed pump, 4.92 lpm (1.3 gpm), was used to simulate an actual installation.

Collector 3 at 50° to Horizontal, Increased Flow Rate

Increasing the flow rate of the heat transfer fluid, in theory, should increase the efficiency of a panel of evacuated tubes as it maintains a larger temperature difference across the manifold by removing heat energy at a greater rate. This increase in flow rate was accomplished by running the Astro3-Spreed circulation pump on its highest setting, corresponding to a flow rate of 5.58 lpm (1.475 gpm) in this setting. The efficiency loss or gain, if applicable, was compared to the standard efficiency obtained in 3.1.2.

Collector 4 at 90° to Horizontal, Low Flow Rate

The efficiency of a panel mounted at an angle of 90° to the horizontal is of interest to determine the feasibility of creating solar collector walls, with the collectors mounted flush with the wall to reduce the possibility of snow accumulation on and between the tubes, which could prove to be difficult to remove on large, tall walls. The rationale for this test was to evaluate the potential for vertical installation of collectors within a south-facing wall in a residential, commercial or industrial application. The intermediate pump flow rate of the Grundfos UPS 15-58 FC circulation pump, 6.34 lpm (1.675 gpm), was used. The efficiency loss or gain, if applicable, was compared to the standard efficiency obtained in 3.1.2.

It is expected that the efficiency of the vertical collector will be greater than that of the control during the winter months due to more direct incident solar radiation. This may be supported by the findings of Budihardjo and Morrison (2009), who although they did not test a vertical panel, found that as the inclination of the collector was increased to 45°, the annual savings during the winter months was 12% higher than when the collector was mounted at 22°.

Collector 3 at 50° to Horizontal, Intermediate Flow Rate, 16 Tubes Removed

As previously mentioned, through plotting the temperature of the condenser ends as a function of location within the manifold it should become apparent, if the plot plateaus, whether or not the efficiency of the collector is a function of the number of tubes per collector. To verify this theory, 16 adjacent tubes, half of the total number of tubes in a full collector, were removed from the manifold and once again the efficiency of the panel was measured. The intermediate pump flow rate of the Armstrong Astro 30-3-Speed pump, 4.92 lpm (1.3 gpm), was used along the length of the manifold. The difference between the temperature of the condenser ends and that of the heat transfer fluid is directly related to the efficiency of the condenser–manifold interface.

Efficiency Measurement Procedures

The efficiency of the panels was evaluated using ASHRAE Standard 93-2003. As previously mentioned this approach was considered to be appropriate since the water-propylene glycol heat transfer fluid did not change state. The standard defines the solar collector efficiency as:

$$\eta_g = \frac{\text{actual useful energy collected}}{\text{solar energy intercepted by the collector gross area}} \tag{1}$$

that is represented mathematically as:

$$\eta_g = (\dot{m} c_p (t_{f,e}\ t_{f,i})/A_g G_t) \tag{2}$$

The mass flow rate of the heat transfer fluid, , was derived from the flow rate as follows;

$$\dot{m} = \rho Q \tag{3}$$

The density of the heat transfer fluid was derived from the specific gravity as measured using a hydrometer. The average value for the four systems was then converted into density units.

The solar radiation was measured with the horizontally mounted pyranometer was adjusted to reflect the actual global solar irradiance incident upon the aperture plane of collec-

tors. The ratio of beam radiation on the tilted surface to that on a horizontal surface, R_b, was determined (Duffie and Beckman, 2006) (Figure 5).

$$R_b = \frac{G_{b,T}}{G_b} = \frac{G_{b,n}\cos\theta}{G_{b,n}\cos\theta_z} = \frac{\cos\theta}{\cos\theta_z} \tag{4}$$

The angle of incidence, θ, is the angle between the beam radiation on a surface and the normal to that surface. The Zenith angle, θ_z, is defined as the angle between the vertical and the line to the sun, which is to say, the angle of incidence of beam radiation on a horizontal surface. β, the slope of the collector, is the angle between the plane of the surface in question and the horizontal.

The following relationship can be used to calculate the angle of incidence of beam radiation on a surface, θ (or θ_z), when certain other angles are known (Duffie and Beckman, 2006).

$$\begin{aligned}\cos\theta = {} & \sin\delta\sin\phi\cos\beta - \sin\delta\cos\phi\sin\beta\cos\gamma \\ & + \cos\delta\cos\phi\cos\beta\cos\omega + \cos\delta\sin\phi\sin\beta\cos\gamma\cos\omega \\ & + \cos\delta\sin\beta\sin\gamma\sin\omega\end{aligned} \tag{5}$$

Further, the declination, δ, may be approximated by the following (Duffie and Beckman, 2006):

$$\delta = 23.45\sin\left(360\frac{284+n}{365}\right) \tag{6}$$

Data were collected every 5 minutes, 24 hours a day, for approximately a year and a half. Data were downloaded on approximately a biweekly basis. Files were saved by date and time of download. The data analysis and reduction was done using Intercooled Stata 9.0 for Macintosh.

The data sets resulting from the data reduction in Stata were copied into Microsoft Excel 2004 for Mac and used to generate the graphs presented in the Results and Discussion Section to follow. Some further manipulation in Excel was required to produce the desired graphs. In particular, mean daily solar irradiance and efficiency were further reduced to mean monthly solar irradiance and efficiencies for each collector configuration.

RESULTS AND DISCUSSION

For efficiency, the scale range is 0–100 %, the minimum and maximum efficiencies. For solar irradiation, the scale ranges from 0–1400 W/m^2, the minimum and just past maximum solar irradiation levels. These scale ranges have been implemented on each graph, to provide a more appropriate depiction of the results without visually skewing the trends with adjusted scales. Therefore, each graph can be directly compared to others of its type.

The following abbreviations were used:

C1 = Collector 1 (Either uncovered or covered with Suntuf panel)

C2 = Collector 2 (Control)

C3 = Collector 3 (Either with increased flow rate or with 16 tubes removed)

C4 = Collector 4 (Vertical)

E1 = Efficiency of Collector 1

E1 (Uncovered) = Efficiency of Collector 1 prior to the installation of the Suntuf Panel

E1 (Covered) = Efficiency of Collector 1 following the installation of the Suntuf Panel

E2 = Efficiency of Collector 2

E3 = Efficiency of Collector 3

E3 (Flow Rate Increased) = Efficiency of Collector 3 with the flow rate increased

E3 (16 Tubes Removed) = Efficiency of Collector 3 following removal of 16 tubes

E4 = Efficiency of Collector 4

Comparison of Mean Monthly Collector Efficiencies to the Control Collector

To observe the relationship, if any, between efficiency and solar irradiance, a scatterplot of efficiency of the control collector (collector 2), calculated using Equation 2, as a function of solar irradiance was produced (Figure 4). There is no obvious simple geometric correlation, such as linear or exponential, between the two variables. The distribution indicates a density or clustering of points on the low end of the efficiency scale across a wide range of solar irradiance values. The plotted points take on a somewhat negative association with each other; high efficiency values appearing to be more prominent at low- to mid-range irradiance values, and with high irradiance values resulting in lower efficiencies. It is apparent that high efficiencies are not as prominent as those below approximately 20% and that solar irradiance dwindles past approximately1000 W/m^2.

FIGURE 4. Efficiency of collector 2 (Control) as a function of solar irradiance.

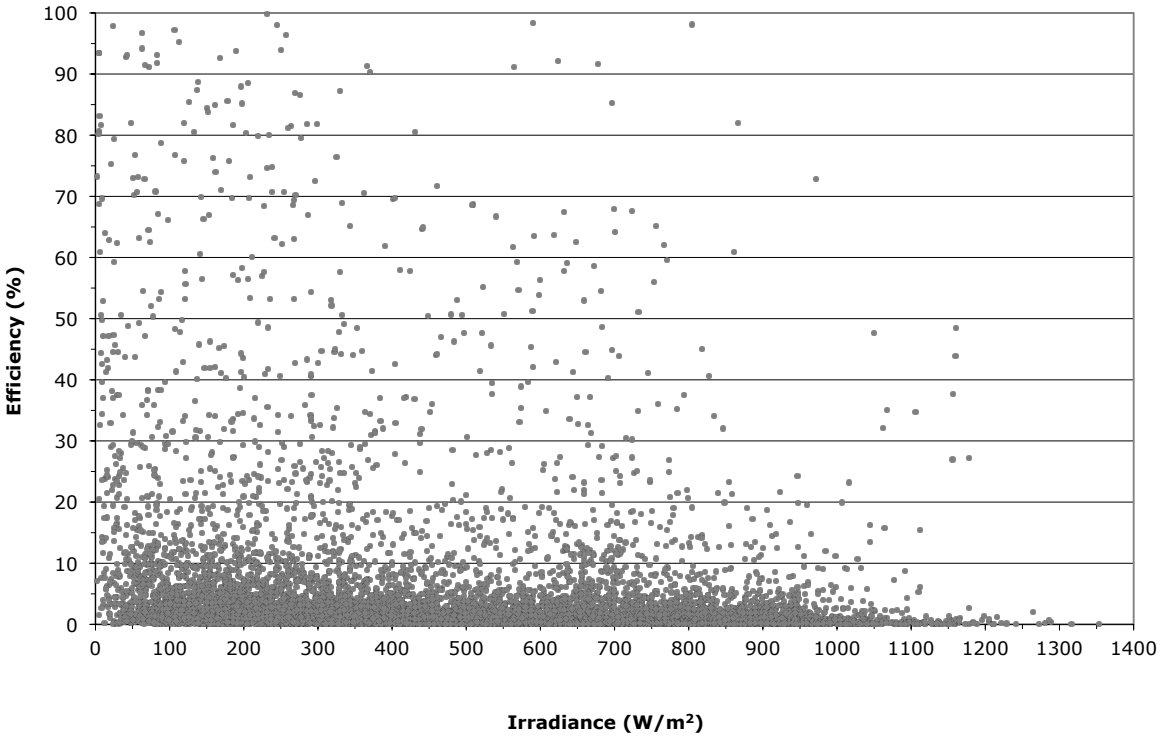

In Figure 5, mean monthly irradiance and mean monthly efficiency for the control collector configuration were plotted as a function of time to again observe the relationship, if any, between collector efficiency and irradiance. The line of mean monthly efficiency indicates that, in general, efficiencies tend to decrease as spring progresses to summer, with summer having the lowest overall efficiencies, then increase through fall, with winter having the highest overall efficiencies. The line of mean monthly irradiance indicates that, in general, solar irradiance tends to increase as spring progresses to summer, with summer having the highest overall irradiance, then decreasing through fall, with winter having the lowest overall irradiances. This is consistent with solar irradiance expectations as reported by Duffie and Beckman (2006). The greatest mean monthly solar irradiance was measured to be approximately 600 W/m^2 in July of 2009.

Figure 6 overlays the efficiency results from each collector onto one graph for efficiency as a function of time. Important dates are noted on the graph, particularly the date that Collector 1 was covered with the Suntuf panel (June 21, 2009), and the date that the flow rate was returned to intermediate speed and 16 tubes were removed from Collector 3 (January 2, 2010). The purpose of overlaying these results is to determine which collectors outperform the others and rank them accordingly. The efficiencies tend to be within less than 5% of each other, suggesting that the different collector configurations have minimal effect on efficiency. However, in general, it appears that the covered collector (C1) performed worse than the others more often than not. The vertical collector (C4) tended to outperform others during the winter months, but fell in line with the covered collector (C1) in the summer. Collector 3, with increased flow rate and the control (C2), fell somewhere in the middle.

FIGURE 5. Mean monthly efficiency and mean monthly solar irradiance for collector 2 (Control) as a function of time of year.

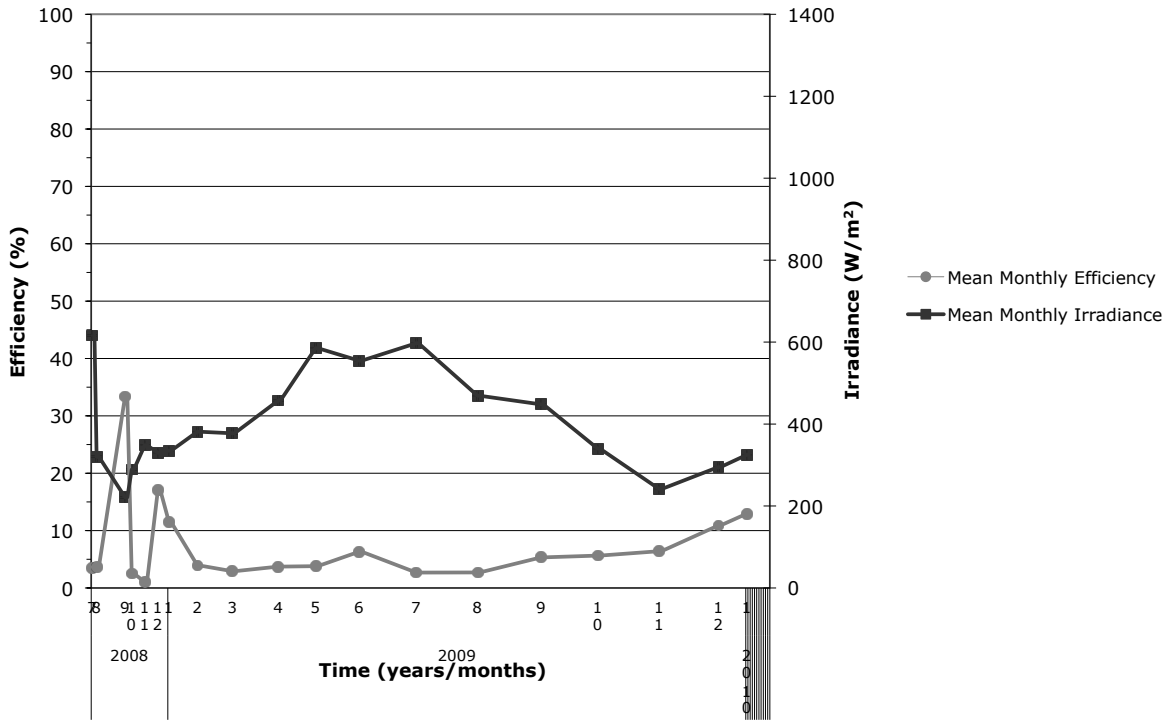

FIGURE 6. Comparison of collector efficiencies as function of time of year.

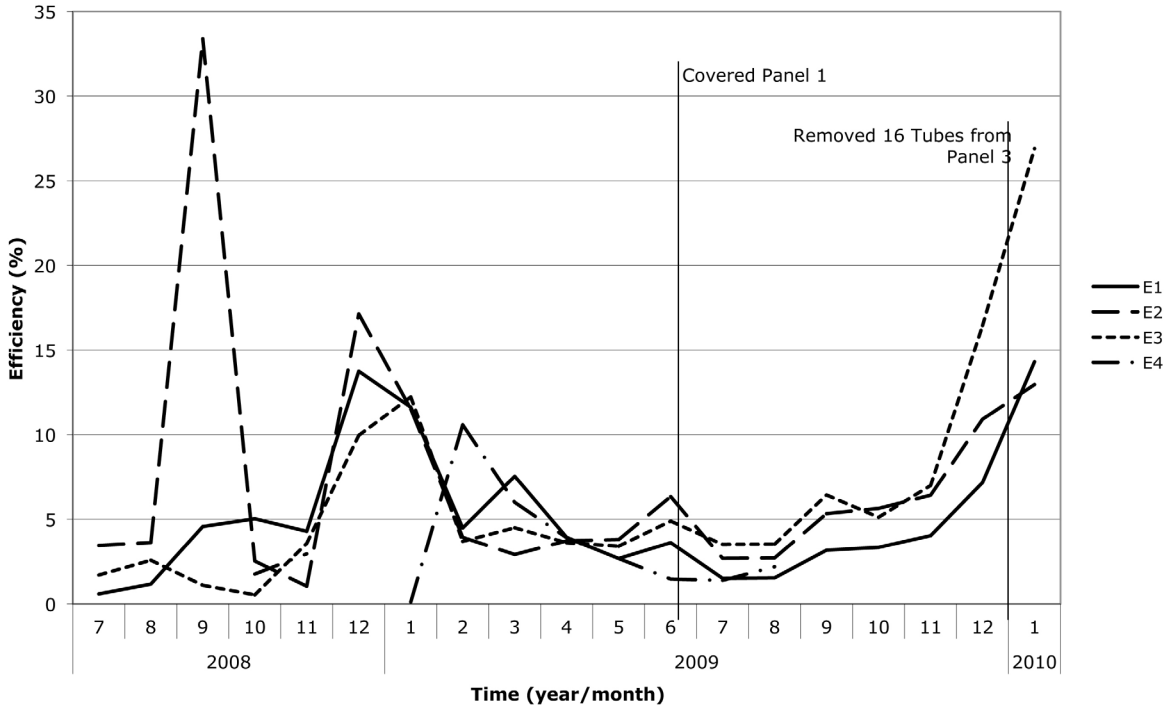

Figure 7 compares the mean monthly efficiency of Collector 1, installed at 50° to horizontal, intermediate flow rate, uncovered and covered to Collector 2, the control. The date that the Suntuf Panel was installed over the collector, June 21, 2009, is indicated with a labeled vertical line. Up until the point of installation of the cover, the two collectors performed in a fairly similar manner. Initially, in July through August of 2008 the control performed slightly better; October and November of 2008 saw the reverse. In general, the outperforming collector oscillated between the control and the uncovered collector, within a margin of less than 5% efficiency (except for the one outlier for the control in August of 2008, when its mean monthly efficiency bolted up to approximately 34%), until the time of cover installation. At this point the control consistently outperformed the covered collector, until January 2010.

These results were expected. The Suntuf cover will restrict the transmittance of solar radiation to the evacuated tubes, and thus cause a decline in performance, as less energy is available to the collector to convert to heat.

According to the mathematical expression used to calculate panel efficiency (Equation 2), as mass flow rate, and therefore volume flow rate, increases, the collector efficiency should also increase, all else being equal. Figure 8 compares the mean monthly efficiency of Collector 3, installed at 50° to horizontal, increased flow rate with to Collector 2, the control. In general, the outperforming collector oscillated between the control and collector 3, within a margin of less than 10% efficiency (except for the one outlier for the control in August of 2008, when its mean monthly efficiency bolted up to approximately 34%). In November of 2009 the efficiency of collector 3 began to rise steeply.

FIGURE 7. Comparison of mean monthly efficiencies of collector 1 (uncovered then covered) to the mean monthly efficiencies of collector 2 (control).

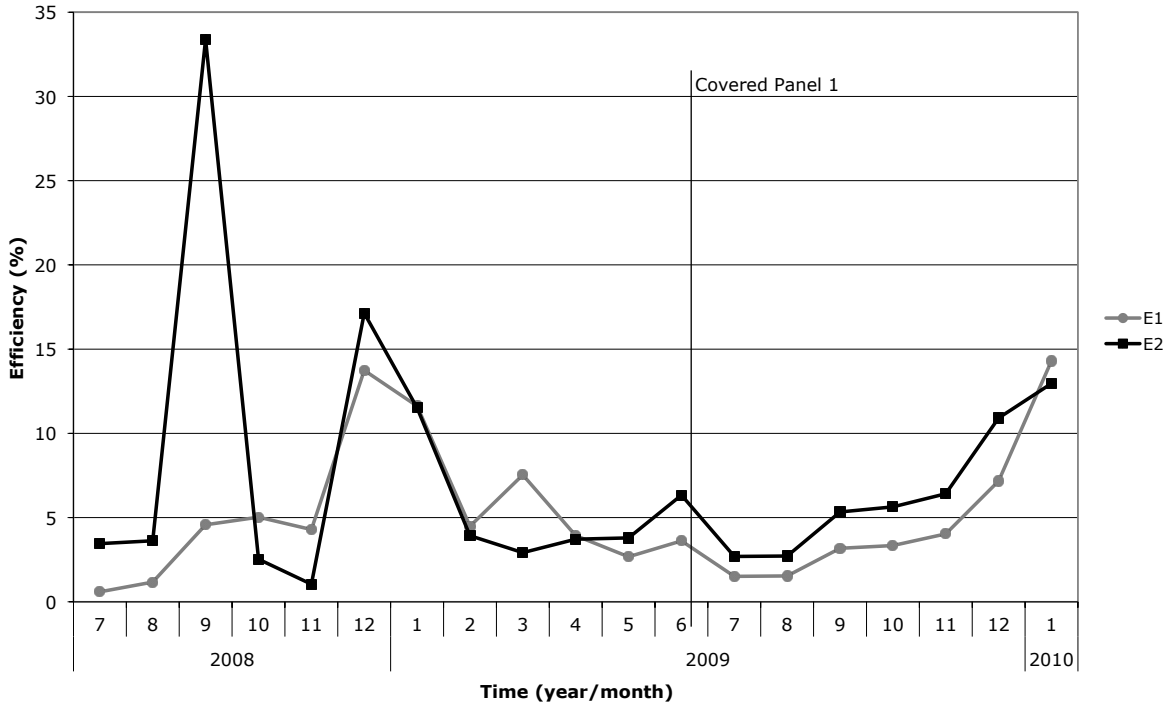

FIGURE 8. Comparison of mean monthly efficiencies for collector 3 (increased flow rate then 16 tubes removed) to the mean monthly efficiencies of collector 2 (control).

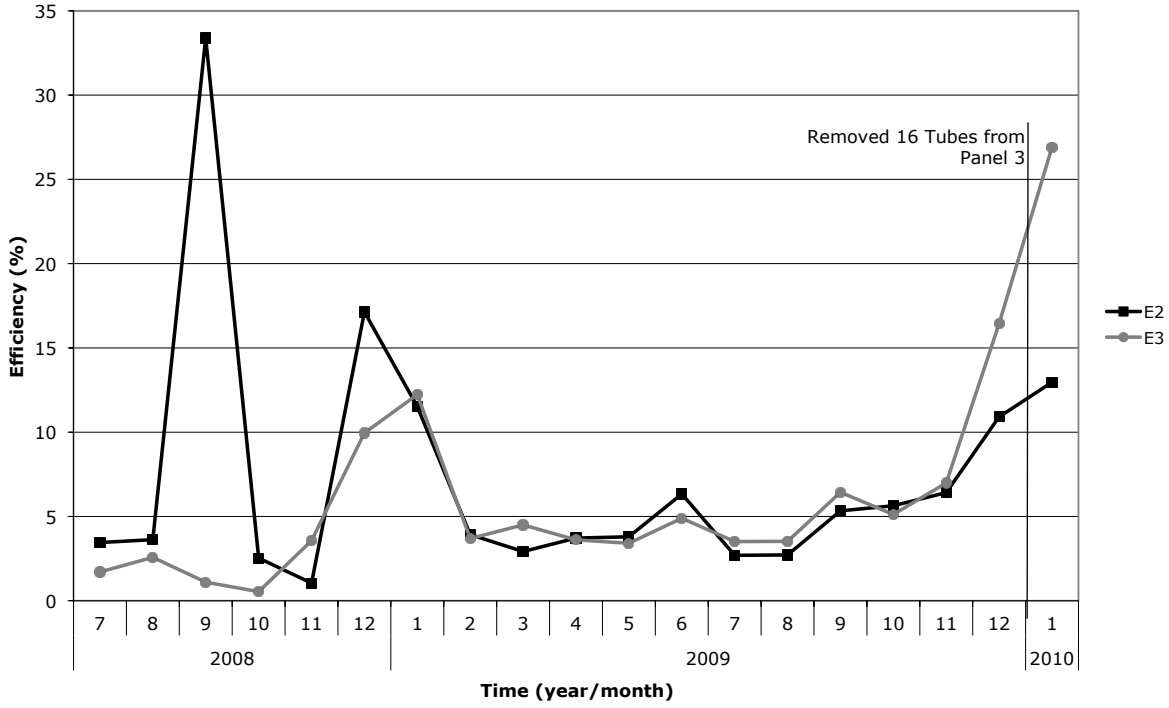

FIGURE 9. Comparison of mean monthly efficiencies for collector 4 (vertical) to the mean monthly efficiencies of collector 2 (control).

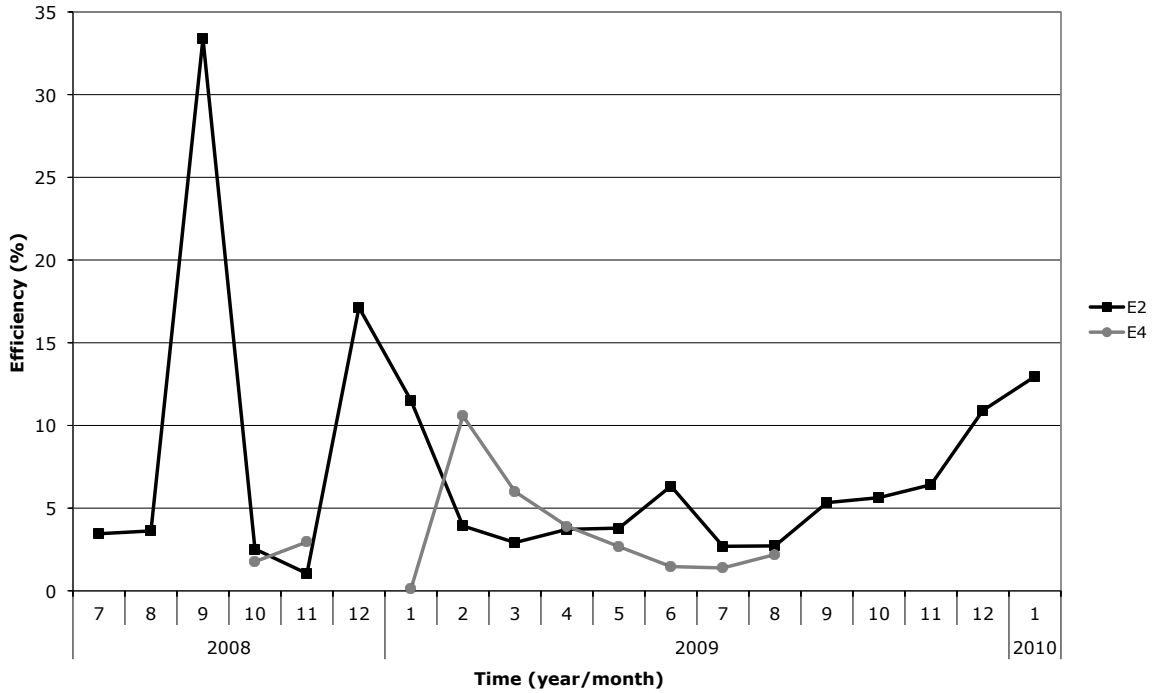

It was expected that collector 4, installed at 90° to horizontal, standard flow rate would outperform the control in the winter months since the 90-degree installation angle would be better suited to the winter sun angle. The data collection for this collector was somewhat sporadic due control malfunctions and the eventual inability to repair the system (September 2009). The best data for comparison is between the months of January to September of 2009. During this time collector 4 did perform as expected, with greater efficiencies than the control during the winter months and the opposite in the summer (Figure 9).

OVERALL COLLECTOR PERFORMANCE ANALYSIS

Through observation of each of the collector configurations above, a few consistent trends were noted. Each plot of efficiency as a function of irradiance showed a similar distribution: the overall form of points indicates a density or clustering of points on the low end of the efficiency scale across a wide range of irradiance values. In general, the plotted points take on a somewhat negative association with each other; high efficiency values appearing to be more prominent at low- to mid-range irradiance values, and with high irradiance values resulting in lower efficiencies. There is no obvious simple geometric correlation between the two values.

The mean daily and monthly efficiency of each collector was plotted as a function of time and again displayed similar trends. Although the mean daily efficiencies varied, the line of mean monthly efficiency indicated that, in general, efficiencies tended to decrease as spring progresses to summer, with summer having the lowest overall efficiencies, then increase through fall, with winter having the highest overall efficiencies.

It should be noted here that for the purposes of this research project the authors believe that, the term "effectiveness" could be substituted for "efficiency" since the evaluation was based solely on collector system performance. Equation 2 represents a theoretical relationship between solar irradiation, flow rate, inlet and outlet temperatures, collector area, etc., under optimal, controlled laboratory conditions. The efficiencies measured here were subject to uncontrollable variables and environmental conditions. Thus, the term "effectiveness" may be more appropriate in describing collector system performance. Where "system" refers to the evacuated tube, manifold, and heat dissipation assembly.

The mean daily and monthly irradiance for each collector was plotted as a function of time, for the same points and duration used for the mean daily and monthly efficiency plots. Although the mean daily irradiances varied, the line of mean monthly irradiance indicated that, in general, solar irradiance tended to increase as spring progresses to summer, with summer having the highest overall irradiance, then decreasing through fall, with winter having the lowest overall irradiances.

Finally, the plots of mean monthly irradiance and efficiencies for each collector configuration showed that the highest efficiencies and lowest irradiances occurred in the winter months, while the lowest efficiencies and highest irradiances occurred in the summer months.

The graphs also displayed outliers during the same dates. In particular, outliers were common in August and December of 2008. December had the most obvious and consistent outliers. Specifically, there was a dip in mean monthly irradiance and an increase in efficiency. This could be due to the lack of data points available in the month of December, where a few lower than usual measurements have skewed the entire mean.

The findings above suggest that evacuated tube collector efficiency could be inversely related to solar irradiance, although the reverse may be expected. Since solar irradiance is strongest in the summer, it may be expected that collector output would also be most efficient during this time. After re-examination of the mathematical expression used to calculate panel efficiency (Equation 2), an alternate explanation is found. Note that as the ΔT in the numerator decreases so too does collector efficiency. The measured ΔT for each collector was smallest in the summer months due to warmer and more equal ambient indoor and outdoor temperatures. During the winter months the strawbale building is heated, and maintains a temperature well above freezing, while outside the ambient temperature could dip in the range of –30 to –40°C with including wind chill. To obtain the greatest difference in temperature, ΔT is measured between the inlet of the manifold, the coldest possible location on the source, and the outlet of the fin-tube, the coldest possible location on the load. Thus, due to environmental conditions, the largest ΔT occurs during the colder seasons. This also indicates that collector efficiency is related to storage capacity of the entire system and ultimately the maintenance of a large ΔT.

Furthermore, if the mean temperature of the fluid in the manifold is substituted for $t_{f,e}$ in Equation 2, and if $t_{ambient}$ is substituted for $t_{f,I}$ in the same equation, the relationship between ambient outdoor temperature, heat transfer fluid temperature and efficiency is apparent. Greater outdoor ambient temperatures result in a smaller ΔT, and thus lower collector efficiency, as observed above.

In addition, the efficiency of the evacuated tube collectors could be limited by the various heat transfer mechanisms inherent in the design. Ultimately, heat can only be transferred as fast as the conductance of the material or fluid will allow. That being said, it may not matter how much solar radiation is available for the taking, if in fact only "X" W/m^2 is useful at

any given time. If this is the case, then collector performance is less dependent upon solar radiation and perhaps more dependent upon the intermediate efficiencies of heat transfer, first between the air space and the copper heat pipe, then between the copper condenser end and the copper manifold seat, then from the manifold to the heat transfer fluid, and so on. The authors believe that instead of referring to efficiency that one needs to consider the overall "effectiveness" of the system, taking into account all of the various components. If, for example, the storage capacity of the system is limited then this will limit the effectiveness of the system regardless of how efficient the collector system may be.

This still leaves the question of how, if at all, solar irradiance and collector efficiency are related. Again, looking at the mathematical expression used to calculate panel efficiency (Equation 2), it is noted that, all else being equal and holding delta T constant, if solar irradiance increases in the denominator, then a lower efficiency can be expected. Unfortunately with the data collected, ΔT could not be held constant, and so this relationship could not be confirmed empirically.

CONCLUSIONS

The purpose of this research program was to measure the efficiency of evacuated tube solar collectors under various operating conditions. These conditions included the angle of inclination towards the incident solar radiation, heat transfer fluid flow rate, glazing installation, and the number of evacuated tubes were of particular interest based on design and installation consequences encountered in practice.

From a practical and architectural point of view, there are a number of possible installation scenarios for evacuated tube collectors that may be more or less appropriate under different environmental, structural, and aesthetic restrictions. This research set out to determine under which conditions different collector configurations would be most appropriate.

The findings indicated that efficiency varied by approximately 5% in general between the different collector configurations, as observed from the overlay graph of results.

That being said, it was observed that covering the collector with a polycarbonate sheet will slightly reduce its efficiency, though hardly enough to be of concern in situations where the benefit would outweigh the slight decrease in performance.

Vertical installations were found to be slightly more efficient than others during the winter months, and slightly less during the summer. This may not be an issue in situations where the demand for heat is greatest in the winter, and heat storage capacity in the summer is a concern. In this case, the best use of the collector would be made in the winter when the load is available, and the decreased efficiency in the summer would not be missed since there would not necessarily be a load available to displace the heat.

As Equation 2 suggests, increasing the mass flow rate, and thus the volume flow rate, should cause an increase in collector efficiency. This was observed to be consistent in Collector 3.

While the efficiency of a collector may be evaluated it is the entire system that affects how the captured solar energy may be utilized. Instead of looking only at the collector efficiency developing a measure of system effectiveness would seem appropriate.

ACKNOWLEDGEMENTS

The authors would like to thank Manitoba Hydro for financial support, the Biosystems Engineering technicians and Alternative Village team for their assistance.

REFERENCES

American Society of Heating, Refrigerating and Air-Conditioning Engineers, Inc. 2003. Methods of testing to determine the thermal performance of solar collectors. ANSI/ASHRAE Standard 93-2003.

Budihardjo, I. and G.L. Morrison. 2009. Performance of water-in-glass evacuated tube solar water heaters. *Solar Energy* 83:49–56.

Carvalho, M.J. and D.J. Naron. 2001. Comparison of test methods for evaluation of thermal performance of preheat and solar-only factory made systems. *Solar Energy* 69:145–156.

Canadian Standards Association. 1988a. Solar domestic hot water systems (liquid to liquid heat transfer), CAN/CSA-F379.1-88.

Canadian Standards Association. 1988b. Solar collectors, CAN/CSA-F378-87.

Duffie, J.A. and W.A. Beckman. 2006. *Solar Engineering of Thermal Processes,* 3rd edition. Hoboken, New Jersey: John Wiley and Sons Inc.

El-Nashar, Ali M. "The effect of dust accumulation on the performance of evacuated tube collectors." *Solar Energy* 53.1 (1994): 105+. *Global Reference on the Environment, Energy, and Natural Resources*.

Kalogirou, S.A. 2004. Solar thermal collectors and applications. *Progress in Energy and Combustion Science* 30:231–295.

Kemp, W.H. 2005. Space heating and cooling with renewable energy. In *The Renewable Energy Handbook*, 159–233. Tamworth, Ontario: Aztext Press.

Marshall, R. 1999. A generalized steady state collector model including pipe losses, heat exchangers, and pump powers. *Solar Energy* 66:469–477.

Mathioulakis, E. and V. Belessiotis. 2001. A new heat-pipe type solar domestic hot water system. *Solar Energy* 72:13–20.

Morrison, G.L., I. Budihardjo and M. Behnia. 2004. Water-in-glass evacuated tube solar water heaters. *Solar Energy* 76:135–140.

Sibbitt, B., T. Onno, D. McClenahan, J. Thornton, A. Brunger, J. Kokko and B. Wong. The Drake Landing solar community project – early results. 2007. Ottawa, Canada: CANMET Energy Technology Centre, Natural Resources Canada; Almonte, Canada: Gagest Inc.; Madision, USA: Tess; Mississauga, Canada: Bodycote Testing Group; Kitchener, Canada: Enermodal Engineering; Ottawa Canada: SAIC Canada.

Sharma, S.D., T. Iwata, H. Kitano and K. Sagara. 2004. Thermal performance of a solar cooker based on an evacuated tube solar collector with a PCM storage unit. *Solar Energy* 78:416–426.

Weiss, W. 2003. Solar Heating Systems for Houses—A Design Handbook for Solar Combisystems, James and James Pub., London, UK. ISBN 1902916468.

APPENDIX

NOMENCLATURE

A_g = gross collector area, m^2
c_p = specific heat of the heat transfer fluid, J/(kg·°C)
G_t = global solar irradiance incident upon the aperture plane of collector, W/m^2
$G_{b,T}$, $G_{b,,}$ $G_{b,n}$ = are defined in Figure 5 below, W/m^2
$\dot{m}$ = mass flow rate of the heat transfer fluid, kg/s
R_b = the ratio of beam radiation on the tilted surface to that on a horizontal surface
$t_{f,e}$ = temperature of the heat transfer fluid leaving the collector, °C
$t_{f,i}$ = temperature of the heat transfer fluid entering the collector, °C
$t_{ambient}$ = outdoor ambient temperature, °C
β = Slope, the angle between the plane of the surface in question and the horizontal; $0° \le \beta \le 180°$.
δ = Declination, the angular position of the sun at solar noon with respect to the plane of the equator, north positive; $-23.45° \le \delta \le 23.45°$.
ϕ = Latitude, the angular location north or south of the equator, north positive; $-90° \le \phi \le 90°$.
γ = Surface azimuth angle, the deviation of the projection on a horizontal plane of the normal to the surface from the local meridian, with zero due south, east negative, and west positive; $-180° \le \gamma \le 180°$.
η_g = collector efficiency based on gross collector area, %
θ = Angle of incidence, the angle between the beam radiation on a surface and the normal to that surface.
θ_z = the Zenith angle, degrees
ω = Hour angle, the angular displacement of the sun east or west of the local meridian due to rotation of the earth on its axis at 15° per hour; morning negative, afternoon positive.

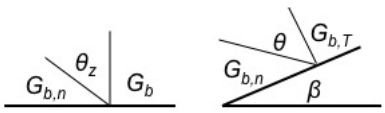

Solar Angle Relationships